Mis-regulation of GSK-3β causes axonal microtubule curling through Shot and Tau

Andre Voelzmann[2,3], Lubna Nuhu-Soso[1], Alex Roof[1], Sanjai Patel[2], Hayley Bennett[5], Antony Adamson[5], Marvin Bentley[4], Gareth J. O. Evans[1], Ines Hahn[#1,2]

1) York Biomedical Research Institute, Department of Biology, University of York, York, UK
2) Manchester Academic Health Science Centre, Faculty of Biology, Medicine and Health, School of Biology, University of Manchester, Manchester, UK
3) Department of Biology, University of Hull, Hull, UK
4) Department of Biological Sciences and the Center for Biotechnology and Interdisciplinary Studies, Rensselaer Polytechnic Institute, Troy, NY
5) Genome Editing unit, Faculty of Biology, Medicine and Health, School of Biology, University of Manchester, Manchester, UK

Running title**:** Dysfunctional GSK-3β disrupts microtubule organisation in axons

Key words: *Drosophila*, GSK-3β, neurodegeneration, axons, cytoskeleton, microtubules

author for correspondence:
Ines Hahn
The University of York
York Biomedical Research Institute
Department of Biology
Heslington, York YO19 4AU
Ines.Hahn@york.ac.uk

Abstract

Glycogen Synthase Kinase 3β (GSK-3β) is a key coordinator of neuronal development and maintenance; overactive GSK-3β is linked to neurodevelopmental and -degenerative diseases making it a highly promising therapeutic target. One of GSK-3β's key roles in neurons is to coordinate the cytoskeleton by directly phosphorylating microtubule binding proteins. However, how GSK-3β orchestrates the activities of a range of microtubule regulators, to jointly maintain microtubule bundles is not well understood. We study the function of GSK-3β using fly primary neurons, a uniquely tractable system which has allowed us to unravel the function of >50 cytoskeletal regulators in the past. Here we report a novel function of GSK-3β. We find that kinase activity needs to be tightly regulated to maintain parallel microtubule bundles in axons. Functional up- as well as down-regulation of GSK-3β leads to axons forming pathological swellings where microtubule bundles disintegrate into criss-crossed curling microtubules. Mechanistically, we have identified Shot and Tau as key GSK-3β targets, providing a means to change microtubule behaviours in a time and location-specific manner. By modifying the ability of Shot and Tau to attach to microtubules and Eb1, both hyperactivity as well as inhibition of GSK-3β leads to the loss of Eb1-Shot-mediated guidance of polymerising microtubules into parallel bundles, thus causing disorganisation. Our findings provide new explanations how overactivity of GSK-3β could lead to neurodegeneration in neurodegenerative diseases and why global inhibition of GSK-3β has not been successful in clinical trials for those disorders.

Introduction

Glycogen synthase kinase-3β (GSK-3β) is a key regulator of neuronal development and

maintenance. It is required for key steps of neuronal development, from neurite initiation, to outgrowth, path finding, branching and synapse formation. In the mature brain, it is involved in neuronal plasticity and maintenance [1]. GSK-3β activity impairment leads to changes in axonal outgrowth, dendritic branching, impaired synapse function [2] and plasticity [3] causing neurodevelopmental (Autism Spectrum Disorder [4]) and mental disorders (depression, mood disorders and schizophrenia [1,5]). Furthermore, overactivity of GSK-3β is tightly linked neurodegenerative disorders such as dementia (Alzheimer's Disease, FTD), motor neuron and Parkinson's disease [6,7]) as well as impaired regeneration after injury [8]. However, we do not fully understand how GSK-3β controls neuronal development or how misregulation leads to neurological disorders.

GSK-3β is key coordinator that links numerous signalling pathways and regulates a broad range of cellular processes, from proteostasis, metabolism and transcription to cytoskeletal dynamics [9]. A key function of GSK-3β is to coordinate the activity of a broad range of microtubule regulators, i.e. through phosphorylating and altering their microtubule and tubulin binding properties [10], for example phosphorylation by GSK-3β activates MAP1B [11] and inhibits Tau, CRMP2, APC, CLASP, ACF7 [10 12 13]). Even though many GSK-3β targets have been identified, the principles behind the complex effector system downstream of GSK-3β is not well understood. For example, we lack insight into how GSK-3β fine-tunes and orchestrates the activities of these various microtubule regulators at the cellular level. Even at a fundamental level there is some controversy over whether GSK-3β activity promotes [14,15] or inhibits [16,17] axon growth as well as which downstream targets are key.

Understanding the complex network of microtubule binding proteins that this kinase regulates is important, because the role of GSK-3β in microtubule regulation has been linked to neurodegenerative disorders like dementia. Over the past decade accumulations of the phosphorylated microtubule binding protein Tau has emerged as key hallmarks of Alzheimer's disease (AD). Tau aggregates (neurofibrillary tangles) have been speculated to impair microtubule stability [18] and kinesin-dependent microtubule-based transport processes [19], increased neuroinflammation and synaptic decay. Tau aggregation could lead to neuronal decay through the loss of endogenous Tau function (e.g. microtubule stabilisation, crosslinking and control of microtubule dynamics), a mechanism that has not yet gained much attention. Overall, GSK-3β is a promising therapeutic target, however, numerous attempts over the past three decades to bring GSK-3β inhibitors from bench to bedside have largely failed, because complete inhibition of also GSK-3β leads to neuronal decay [20].

A potential explanation for this could come from a model that the Prokop lab recently proposed [21]. The model of local axon homeostasis proposes that parallel bundles of microtubules are at the heart of nervous system development and maintenance. They are essential to establish axonal and dendritic projections, adapt neuronal cell shape and provide transport routes for synaptic vesicles, RNA and proteins and consequently neuronal function. The model proposes that parallel arrangement is maintained by several molecular mechanisms involving microtubule binding proteins and microtubule-based molecular pathways and that this is crucial for neuronal function and maintenance [21,22]. When those mechanisms are weakened, bundles disintegrate with microtubules displaying intertwined, criss-crossing curls. This can cause the formation of axonal swellings, a hallmark of neuronal decay. Similar swellings have been observed in neuronal disease like Alzheimer's, Parkinson's, Multiple Sclerosis and other neurodegenerative disease [23 24 25 26 27].

Several molecular mechanisms that control microtubule bundling are linked to dynamics of microtubules. Amongst other factors, EB proteins, Tau and Spectraplakins have been found to

play an important role in the growth of microtubules and their guidance into bundles [28]. Spectraplakins, a family of large, actin-microtubule crosslinkers mediate a key mechanism. They are linked to the axonal cortex with their actin-binding N-terminus. Their C-terminus binds Eb proteins that are located at growing ends of microtubules where they guide growing microtubule into parallel bundles [28,29]. This mechanism can be broken in two ways – either by removing Shot or Eb1 [28]. We've previously shown that Tau function ties in with this mechanism. By binding the microtubule lattices Tau helps restricting Ebs to the plus tip. Loss of Tau leads to sequestering of Eb1 to the microtubule lattice, reduction of free Eb1 levels, impaired formation of plus ends and consequently no efficient guidance of microtubules into parallel bundles through Shot [30].

We speculated that mis-regulation of GSK-3β affects the delicate balance of regulators that maintain parallel microtubule bundling by altering the affinity of microtubule regulators for microtubules. To test how GSK-3β activity affects organisation of microtubule bundles and which microtubule coordinators are the key target that regulate axonal microtubules, we used our powerful and tractable *Drosophila* primary neuron cultures. This model was used previously studied the function of >50 cytoskeletal regulators [31,28,30,32, 33, 34], giving us a unique, unified data base from a single model to explored how GSK-3β impacts microtubule networks and which regulators mediate this.

We found that mis-regulation of GSK-3β disrupts the organization of parallel microtubule bundles. GSK-3β activity must be tightly regulated, as both its activation and inhibition lead to the formation of disorganized, curled microtubules in mouse and *Drosophila* neurons. We identified two key microtubule-binding proteins, Short Stop (Shot, a spectraplakin) and Tau, as crucial targets of GSK-3β in this process. We propose that overactivation of GSK-3β reduces Tau binding to microtubules, which disrupts the Shot/Eb1-mediated alignment of polymerizing microtubules into parallel bundles, ultimately causing microtubule unbundling. Furthermore, GSK-3β inhibition seems to directly affect the function of Shot, a microtubule-actin crosslinker, suggesting that Shot's role in guiding polymerizing microtubules relies on its phosphorylation by GSK-3β. We propose these differential effects on the activity of key microtubule regulators and their combined impact on microtubule bundle maintenance is a new mode how hyper- and hypophosphorylation by GSK-3β causes pathology. It furthermore provides an explanation why global GSK-3β inhibition has so had only small therapeutic effects in neurodegenerative disease contexts.

Methods

Fly stocks

Lines for targeted gene expression were *UAS-sgg.S9A* (*UAS-sggCA*; constitutively active (CA) form of Sgg, [35]), *UAS-sgg.A81T (UAS-sgg.DN;* inactive form of Sgg, [36]), *UAS-Eb1-GFP and UAS-shot-Ctail-GFP (EGC-GFP)*[28]. Loss-of-function mutant stocks used in this study were *sgg*^{1} (hypermorphic allele, [37]), *dtau*^{KO} (a null allele; [38], tau-/-), *shot*^{3} (the strongest available allele of *short stop*; [29,39]). Gal4 driver lines used were the pan-neuronal lines *elav-Gal4* (1st and 3rd chromosomal, both expressing at all stages) [40]. The protein trap line used was P{Wee}tau[304] (tauGFP; [41 42]). To induce gene expression with RU486, UAS constructs were expressed using an elavGal4-GeneSwitch driver line (RRID:BDSC_43642, [43 44]). Gene expression was induced by adding 200 mg/mL RU486 to cell culture media. Oregon R stocks, heterozygous crosses of UAS or Gal4 lines with Oregon R or uninduced fly lines were used as controls as indicated.

Generation of Shot-eGFP CRISPR/Cas9 lines

The five C-terminal exons of Shot coding for the C-tail and SxIP sites (shot-RH, FBtr0087621) were excised from the shot genomic region and replaced with fused version of those exons and an additional C-terminal eGFP or a phosphodeficient/mimetic versions following the same strategy, leading to either eGFP-tagged wildtype Shot (*Shot^{WT}-eGFP*) containing a unmodified GSK-3β target site (SRAGSKPNSRPLSRQGSKPPSRHGS), phospho-deficient Shot where Serines where mutated into Alanines (**A**RAG**A**KPN**A**RPL**A**RQG**A**KPP**A**RHG**A**) and phospho-deficient Shot where Serines were mutated into Aspartic Acid residues (**D**RAG**D**KPN**D**RPL**D**RQG**D**KPP**D**RHG**D**). The three Shot coding sequences with eGFP were synthesised as gBlocks (IDT).

Suitable gRNA target sites (5′ gRNA: GGAGGCTCTCGTGCCGGCTC, 3′ gRNA: GCTATAGGAAGCCACCGTTA) were identified by CRISPR optimal target finder [45] and cloned into pCFD5 (Addgene plasmid #73914; [46]) via Gibson assembly (NEB).

CRISPR donor plasmids were cloned with 0.8 kb 5’ and 3’ homology arms amplified from fly genomic DNA into pUC57(Addgene plasmid #51019, RRID:Addgene_51019), flanking the different CTail Shot-eGFP coding sequences, amplified from the above gBlocks. using a three-fragment Gibson assembly . Primer sequences are provided below.

Fragment	Template DNA	Primer(s)	Sequence
1 (5'H)	Fly gDNA	Fragment 1 For	agtcacgacgttgtaaaacgacggccagtgaattctgctgctgcgccgc
		Fragment 1 Rev WT	ggagccggcacgagatccgcctggcgtgagacccgt
		Fragment 1 Rev Mimic	gtcgccggcacgatctccgcctggcgtgagacccgt
		Fragment 1 Rev Mutant	ggcgccggcacgagctccgcctggcgtgagacccgt
2 (cds-eGFP)	gBlocks	Fragment 2 For WT	ctcacgccaggcggatctcgtgccggctcca
		Fragment 2 For Mimic	ctcacgccaggcggagatcgtgccggcgaca
		Fragment 2 For Mutant	ctcacgccaggcggagctcgtgccggcg
		Fragment 2 Rev	aacggtggcttcctattacttgtacagctcgtccatgcc
3 (3'H)	Fly gDNA	Fragment 3 For	gagctgtacaagtaataggaagccaccgttatggct
		Fragment 3 Rev	atctagatgcattcgcgaggtaccacaattttcactttcctattagtttaataacagaac

Constructs were midi-prepped (Bioline) and eluted in ddH2O, before injection into y[1] sc[1] v[1];; {y[+t7.7] v[+t1.8]=nanos-Cas9}attp2 (gift from the University of Cambridge) and selected for eGFP-positive flies. Positive candidates were confirmed by Sanger sequencing.

Drosophila primary cell culture

Drosophila primary neuron cultures followed protocols described previously[30,32,47]: Embryos (stage 11) were incubated with bleach for 90s, sterilized in 70% ethanol (not exceeding 5 min), washed in sterile Schneider’s medium supplemented with 20% fetal calf serum (Schneider’s/FCS; Gibco), and homogenized with micro-pestles in 100 µl dispersion medium (0.005% phenylthiourea, 1% Penicilin/Streptomycin in HBSS medium (SigmaAldrich, [47]) and incubated for 4 min at 37°C. Dispersion was stopped with 200 µl Schneider’s/FCS, cells were

spun down for 4 mins at 650 g, supernatant was removed and cells re-suspended in 30 µl of Schneider's/FCS per cover slip. Usually, three cover slips (technical repeats) were cultured for each condition with 6-8 embryos per coverslip (18-24 for three). 30 µl drops were placed in the centre of culture chambers and covered with a concanavalin A (5 µg/ml) coated cover slip. Cells were allowed to adhere to cover slips for 90-120 min, then turned and grown as a hanging drop culture at 26°C as indicated.

Transfection of *Drosophila* primary neurons followed an established protocol [48]. Steps were identical to the protocol described above up to the dispersion step but the embryo number was increase to 60-75 per 100 µl dispersion medium. Dispersion was inactivated with Schneider's/FCS and cells centrifuged as above. The cell pellet was re-suspended in 100 µl transfection medium. To generate transfection medium, 0.1-0.5 µg DNA in 50 µL Schneider's with FCS and 2 µl Lipofectamine 2000 in Schneider's medium with FCS were mixed and incubated for 20 min to form transfection complexes. The cells were incubated with the transfection mix for 24 hrs at 26°C in tubes. Cells were then centrifuged for 4 mins at 650 g, supernatant was removed and then incubated with dispersion medium for 4 min. Reaction was stopped with 200 µl Schneider's/FCS and cells were spun down again and re-suspended in culture medium and plated out as described above with a density of 25 embryos per cover slip.

Rat hippocampal primary cell culture

Primary hippocampal neurons were cultured as previously described [49]. In short, E18 rat hippocampi were dissected, trypsinised, dissociated, and plated on 18 mm glass coverslips coated with poly-L-lysine. Cultured neurons were grown in N2-supplemented Minimal Essential Medium at 37°C with 5% CO2. Stage 4/5 hippocampal neurons (5-11 DIV respectively) were transfected with Lipofectamine 2000 (Thermo Fisher, Cat# 11668019) following manufacturer's instructions. To image stage 3 neurons, dissociated neurons were electroporated by nucleofection (AMAXA) using standard protocols prior to plating. Cells were allowed to express for 24 h before imaging or fixation.

Immunohistochemistry

Primary neurons were fixed for 30 min at room temperature (4% paraformaldehyde (PFA) in 0.05 M phosphate buffer, pH 7–7.2). For anti-Eb1 stainings ice-cold +TIP fix (90% methanol, 3% formaldehyde, 5 mM sodium carbonate, pH 9; stored at -80°C and added to the cells) [50] was added and cells were fixed for 10 mins at -20°C and then washed in PBT (PBS with 0.3% TritonX). All subsequent staining and washing steps were performed with PBT.

The following staining reagents were used: anti-tubulin (clone DM1A, mouse, 1:1000, Sigma); anti-DmEb1 (gift from H. Ohkura; rabbit, 1:2000)[51]; anti-GFP (rab, 1:500, ab290, abcam); anti-HA (rat, 1:200, 3F10, SigmaAldrich); F-actin was stained with Phalloidin conjugated with TRITC/Alexa647, FITC or Atto647N (1:100; Invitrogen and Sigma). Specimens were embedded in ProLong Gold Antifade Mountant (ThermoFisher Scientific).

Microscopy and data analysis

For standard imaging we used AxioCam 506 monochrome (Carl Zeiss Ltd.) or MatrixVision mvBlueFox3-M2 2124G digital cameras mounted on BX50WI or BX51 Olympus compound fluorescence microscopes. For the analysis of primary neurons, we used the following parameters:

Degree of disorganised microtubule curling in axons was assessed as "microtubule disorganisation index" (MDI; described previously[30,32]) where the area of disorganised curling

was measured with the freehand selection in ImageJ.

The amount of Eb1 at microtubule comets was approximated from Eb1 stainings on microtubule ends by multiplying comet mean intensity with comet length (described here [30]).

Axon length: Using the segmented line tool of Image J, we measured length from cell body to growth cone tip[30,52].

Live microtubule dynamics:

Drosophila: To assess microtubule polymerisation dynamics in *Drosophila* primary neurons expressing Ctail-GFP (EB1-interacting region of Shot [28]), movies were collected with an Andor Dragonfly200 spinning disk upright confocal microscope (Leica DM6 FS microscope frame) using a 100x/1.40 UPlan SAPO (Oil) objective at 26°C. Samples where excited using 488 nm and 561 nm diode lasers via Leica GFP and RFP filters respectively and images collected with a Zyla 4.2 Plus sCMOS camera with a camera (1x gain). Time lapse movies were constructed from images taken at 1 s intervals for 1 min.

Rat: Movies were acquired with an Andor Dragonfly built on a Ti2 (Nikon) with a CFI Apo 60× 1.49 objective (Nikon) and two sCMOS cameras (Zyla 4.2+; Andor) from primary hippocampal neurons at 2 or 11 DIV. The imaging stage, microscope objectives, and cell sample were kept at 37°C. The z-axis drift was controlled by a Perfect Focus System (Nikon). Live movies were recorded for 60 s at one frame per second. Axons were identified with an CF405-conjugated anti-neurofascin antibody (NeuroMab, Cat#: 75-027; Mix-n-Stain CF405S Antibody Labeling Kit; Biotum, Cat#: 92231) in the imaging medium.

We used Kruskal–Wallis one-way ANOVA with *post hoc* Dunn's test or Mann–Whitney Rank Sum Tests to compare groups, and $\chi 2$ tests to compare percentages. All raw data of our analyses are provided as supplementary Excel/Prism files.

<u>Recombinant protein expression and purification</u>

Primers were designed for MAP1B, shot and shot mutant peptide sequences with 5' EcoRI and 3' XhoI sites, annealed and ligated into pGEX-4T-1 (GE Healthcare). Peptide sequences are as follows; ERLSPAKSPSLSPSPPSPIEKT for MAP1B, SRAGSKPNSRPLSRQGSKPPSRHGS for shot and ARAGAKPNARPLARQGAKPPARHGA for shot mutant. Empty pGEX-4T-1 plasmid was used for GST only.

All constructs were expressed in BL21 E. coli at 37°C. Cultures at OD600 = 0.8 were induced with 1 mM Isopropyl β-D-1-thiogalactopyranoside (IPTG) for 3 h at 37°C with shaking at 200 rpm. Bacteria were harvested by centrifugation at 5000 x g for 15 mins at 4°C and pellets were stored at -70°C overnight. Pellets were resuspended in 20 ml of PBS containing 1 mM phenylmethylsulfonyl fluoride (PMSF), 1X protease inhibitor cocktail and 6.65 mg of lysozyme. After incubation on ice for 30 min, 1 % (v/v) Triton X-100 and 5 mM DTT were added followed by 6 x sonication on ice for 30 s on and off for a total of 5 min 30 s at 17 kHz. The lysate was clarified by centrifugation at 12,000 rpm for 30 min at 4°C and the supernatant was incubated with Glutathione Sepharose 4B resin for at least 1 h at 4°C with agitation. Glutathione resin was recovered by centrifugation, washed and protein was eluted in elution buffer (100 mM Tris pH 8.0, 20 mM glutathione, 100 mM NaCl). Purified protein was stored at -70°C until use.

<u>In vitro kinase assays</u>

Constitutively active GSK3β protein was obtained from MRC PPU (Dundee). Rabbit monoclonal thiophosphate ester antibody (clone 51-8) and p-Nitrobenzyl mesylate (PNBM) were obtained

from Abcam (Cambridge, UK). ATPγS was obtained from Biorbyt (Cambridge, UK). All other reagents were obtained from Sigma (Dorset, UK)

Thiophosphorylation assays were performed in 25 µl reaction volumes at 30°C for 3 h. The reactions contained 400 ng of GSK3β, 3 µg of substrate (GST or GST-peptides) and reaction buffer (50 mM HEPES pH 7.5, 10 mM MgCl2, 100 mM NaCl, 1 mM DTT). The reactions were left to equilibrate at 30°C after which ATPγS was added to a final concentration of 1 mM to start the reaction. After 3 h, the alkylating agent, PNBM, was added to a final concentration of 2.5 mM and reactions were left for 2 h at room temperature. Reactions were quenched by addition of 4X Laemmli sample buffer. Samples were separated on a 12.5% SDS-PAGE gel, transferred to PVDF membrane and thiophosphorylation determined by Western blotting with rabbit anti-thiophosphate ester (1:10000) and anti-rabbit-HRP (1:5000) and visualised by enhanced chemiluminescence reagent (ECL). Coomassie stained gels were run alongside to ensure equal loading of substrates. Densitometry was performed on Western blots and Coomassie stained gels using ImageJ.

Results

Activation or inactivation of GSK-3β both lead to unbundling and curling of axonal microtubules in *Drosophila* primary neurons

To evaluate the impact of GSK-3β activity on axonal microtubule organization, we expressed previously characterized GSK-3β mutants in cultured neurons and evaluated microtubule organization. Primary neurons were derived from embryos mutant fly lines overexpressing either dominant-negative (*UAS-sggDN*; A81T mutation [36]) or a constitutively active GSK-3β (CA, *UAS-sggCA*, S9A [36]) using the *elavGal4* driver line. After 6 hours in vitro (HIV), neurons were fixed and immuno-stained for endogenous tubulin to visualize microtubules. Activation or inhibition of GSK-3β caused axon swellings in which microtubules lost their bundled conformation and were arranged into criss-crossing curls (Fig. 1A,C). These observations were reflected in quantifications using the previously established microtubule disorganization index (MDI; area of microtubule disorganisation relative to axon length; see [48]). This quantification measures the fold-increase of microtubule unbundling compared to control neurons. The measurements resulted an MDI of 1.8 for sggCA and 2.1 for sggDN (Fig. 1C). To independently verify the impact of GSK-3β inactivation on microtubule organization, we cultured neurons from a GSK-3β loss-of-function allele (*sgg*^{1}, [53]) or treated neurons with increasing concentrations of the GSK-3β inhibitor lithium (Li, [54]). Those conditions resulted in a significant increase in microtubule unbundling; 1.8-fold in *sgg*^{1}, and up to 3.3-fold with 10mM Lithium (Fig. 1D). To determine if GSK-3β regulation of microtubule organization depends on developmental stage, we analysed neurons expressing sggCA or sggDN for 3 days in culture (3DIV, Fig.1B) and found increased microtubule curling in both conditions (sggCA: 2.5; sggDN: 2.7, Fig.1C). Similarly, we observed significant microtubule unbundling in neurons cultured from larval brains expressing sggCA (MDI: 3.9) or sggDN (MDI: 2.8; Fig.1D). Because both over- and inactivation of GSK-3β resulted in microtubule curling, we interpret these results to mean that GSK-3β activity must be tightly regulated to efficiently maintain microtubule bundles.

We next wanted to understand if microtubule unbundling caused by GSK-3β mis-regulation is only occurring during development or during development as well. To test this, we used an inducible gene-switch (GS) expression system ([55]; see Materials and methods for details): the *elavGS/UAS-sggCA* or *-sggDN* neurons were grown without induction for three days, a stage at which they have long undergone synaptic differentiation [56]. After this period, expression of

UAS-sggCA, -sggDN or elavGS only control was induced via RU486 for one day. Cells were fixed and stained. At this point, microtubule disorganisation in neurons expressing in/active GSK-3β was significantly increased over control neurons (2.7-fold in CA and 2.3-fold in DN neurons, Fig.1E). In a parallel approach, we treated three days old cultured neurons with 10mM Li and observed a similar, 2.3-fold increase of microtubule disorganisation (Fig. 1E). Overall, this indicates that a precise balance of GSK-3β activity is required during development but also during later maintenance to prevent microtubule disorganisation.

Impact of GSK-3β activity on microtubule bundles is evolutionary conserved in rat hippocampal neurons

To assess a potential evolutionary conservation, we analysed the effect of hyperactive and inactive GSK-3β on microtubule bundles in rat hippocampal neurons. We transfected primary neurons either at 1 or 6DIV with active (HA-GSK-3βS9A [57]) or inactive (HA-GSK-3βK85A [58]) GSK-3β and fixed after one or seven days (7DIV) respectively. We find that microtubule unbundling is increased in both conditions: 2.1- and 3.3-fold in neurites of young neurons, respectively, 4.6- and 3.9-fold in dendrites of 7-day old neurons. (Fig. 1F-H). In mature neurons, we measured MDI in dendrites and the percentage of axons with disorganised microtubules. We found an increased from 13 to 44% (hyperactive GSK-3β) and 40% (inactive GSK-3β) respectively (Fig. 1I). This reiterates that a correct balance of GSK-3β activity is required to maintain microtubule bundles and that this is a conserved feature in rat neurons. We next wanted to address underlying mechanisms.

GSK-3β affects Eb1 comet formation and dynamics differentially

Our previous work showed that microtubule bundle arrangement is tightly linked with microtubule polymerisation (Fig.2A, [30]). This is mediated by the spectraplakin Shot which guides polymerising microtubules into parallel bundles. Shot binds cortical actin through its N-terminus and Eb1 through its C-terminus and thereby prevents microtubules from growing towards the cortex and curling up [28]. This mechanism can be broken from both sides. Either through loss of Shot or through depletion of Eb1 from plus ends leading to microtubule curling; we found a clear correlation between Eb1 amounts at plus ends and degree of microtubule curling [30].

GSK-3β affects microtubule polymerisation [16]. We therefore wanted to assess if microtubule unbundling upon in/activation of the kinase is due to impaired microtubule polymerisation through depletion of Eb1 at plus ends. To test this, we analysed the amount of Eb1 at plus ends by staining primary fly neurons expressing inactive/active GSK-3β for endogenous Eb1. We approximated Eb1 amounts at microtubule plus ends by multiplying Eb1 comet length with mean Eb1 intensity (see also [30]) and found that Eb1 amounts at plus ends are affected, however, in opposite directions. In neurons cultured for 6 HIV, Eb1 comets are visibly smaller (Fig.2B) and the amount of Eb1 at plus ends is reduced to 67% when GSK-3β is hyperactive (sggCA, Fig.2C). In contrast, we find a slight but significant increase in Eb1 comets size and amounts expressing inactive GSK-3β (sggDN, Fig.2B,C). In more mature neurons (cultured from larval brains) effects are similar. Eb1 amounts in comets are decreased to 58% when expressing active GSK-3β, however, inactive kinase expression has no impact (Fig.2C). We also observe comparable changes in Eb1 comet dynamics: Eb1 comet velocity as readout for MT polymerisation speed is unaffected upon GSK-3β hyperactivation (CA) and only mildly increased upon GSK-3β inactivation (DN). Eb1 comet lifetime however is reduced (to 58% and 88% respectively) when assessed in live imaging experiments using Shot-Ctail::GFP as a readout [28].

To test evolutionary conservation, we analysed microtubule dynamics in rat hippocampal neurons at 1DIV by co-expressing in/active GSK-3β and Eb3-GFP. Similar to our findings in

3DIV fly neurons, comet sizes and dynamics are affected. GSK-3β^{CA} causes a reduction in comet lengths and velocity to 75% and 73% respectively but does not impact comet lifetime (Fig.2F-I). Co-expressing inactive kinase does not affect comet length or dynamics (speed and lifetime; Fig F-I).

Even though curling of microtubule bundles is increased in both, sggCA and -DN conditions, Eb1 is affected differently: GSK-3β hyperactivation decreases Eb1 amounts and aspects of Eb1 dynamics (lifetime in flies, velocity in rats). Expressing the inactive version slightly increases Eb1 in early fly neurons but does not decrease Eb1 dynamics significantly. This suggests that loss of Eb1 from plus end might provide an explanation for microtubule unbundling when expressing GSK-3β^{CA}, but not GSK-3β^{DN}. Hence, the underlying, evolutionary conserved mechanisms that lead to microtubule unbundling upon hyper- or inactivation of GSK-3β might differ. We next investigated this further focussing on GSK-3β hyperactivity first.

GSK-3β hyperactivation leads to microtubule disorganisation via loss of Tau

The most prominent microtubule regulator targeted by GSK-3β is Tau where phosphorylation of Tau leads to detachment from microtubules. We therefore wanted to establish if loss of Tau is causal in microtubule unbundling. We first wanted to test this by analysing if GSK-3β activity affects Tau localisation along microtubules in primary fly neurons. Using an endogenously tagged Tau-GFP [41], we found that expression of GSK-3β^{CA} led to a 38% reduction in Tau levels along the axon whereas expression of GSK-3β^{DN} had no effect (Fig.3A, A').

We next performed genetic interaction studies to investigate potential functional relationships between Tau and active GSK-3β in microtubule bundling. We used heterozygous condition (i.e. one mutant and one normal copy, *tau*$^{+/-}$) of *tau* to reduce protein levels. This by itself does not display any phenotype at 6HIV (Fig.3B). However, when combined in neurons that simultaneously express active GSK-3β (sggCA) we observe an increase in microtubule unbundling from 2.5-fold to 4.6-fold (Fig.3B) suggesting that they might function in a common pathway.

To further test whether the functions of Tau and active GSK-3β regulate the assessed microtubule properties through the same or independent parallel mechanisms, we performed epistasis experiments [59]. For this, we expressed active GSK-3β in homozygous *tau* mutants and asked whether this condition enhances phenotypes over the individual conditions (indicating a parallel mechanisms), or whether they show no further increases (indicating a hierarchical organisation). Loss of Tau led to a 1.6-fold, expression of active GSK-3β alone to a 1.9-fold increase in microtubule unbundling which was not significantly further increased when combined (2-fold; Fig. 3C). Those results are consistent with a model where loss of Tau microtubule association could be the key mechanism when GSK-3β is active.

We previously showed that loss of Tau leads to microtubule unbundling due to Tau's role in preventing Eb1 from binding the microtubule lattice. When Tau is lost (or not able to bind microtubules), Eb1 is sequestered to the microtubule lattice away from the plus end which leads to smaller Eb1 comets. Consequently, Shot is not able to bind plus ends efficiently leading to loss of Shot-mediated guidance of growing microtubules into parallel bundles [30].

To assess if hyperactive GSK-3β leads to microtubule unbundling through this mechanism, we tested if constitutively active GSK-3β expression affects Eb1 localisation along the microtubule shaft. We analysed this in fixed cells expressing active GSK-3β and controls stained for endogenous Eb1. We found that concomitant to a decrease of Eb1 localised at microtubule plus

ends (Fig2C), the mean intensity of Eb1 along the microtubule shaft (areas without comets) is increased 1.3-fold when active GSK-3β is expressed (Fig.3D). We had previously shown that increasing Eb1 levels by co-expressing Eb1::GFP can restore Eb1 to the plus tip and rescue microtubule curling in [30]. This approach also rescued microtubule unbundling caused by GSK-3β hyperactivity (Fig.3E). These effects were specific for Eb1; no improvement of the *GSK-3β^{CA}* phenotype was observed when expressing the plus end binding Shot-Ctail::GFP (EGC-GFP, Fig 3E). Overall, this is consistent with our observations in homozygous *tau* mutants [30] and we therefore propose that sequestering of Eb1 towards the lattice binding due to loss of Tau is causing microtubule unbundling when GSK-3β is active (Fig.3F).

In contrast, our data point towards inactive GSK-3β causing microtubule unbundling through a different mechanism. Expression of *GSK-3β^{DN}* had no effect on Tau localisation in neurons (Fig.3A), Eb1 plus end or lattice binding are not affected (Figs.2C, 3D) and there is no genetic interaction between GSK-3β^{DN} expression and heterozygous *tau* mutants (Fig.3B). Furthermore, in our epistasis experiment expression of GSK-3β^{DN} increases microtubule unbundling in homozygous tau mutants above the levels of individual conditions, from 1.7-fold (*tau* mutants) and 1.4-fold (GSK-3β^{DN}) to 3.2-fold (Fig.3C). This points towards a parallel mechanism of GSK-3β inactivation causing microtubule unbundling which we explored next.

<u>Shot and GSK-3β genetically interact</u>

The most prominent mediator of microtubule bundling is Shot which guides polymerising microtubules into parallel bundles by binding cortical actin with its N-terminus and Eb1 at growing microtubules with its C-terminus. Importantly, microtubule binding of the mammalian spectraplakin ACF7 was shown to be regulated by GSK-3β in skin stem cells where phosphorylation of the C-terminus of ACF7 leads to detachment from microtubules [13].

We wanted to test first if GSK-3β and *shot* genetically interact. Reducing Shot levels to 50% while expressing active or inactive GSK-3β led to a significant increase in microtubule unbundling compared to individual conditions (Fig.4A). Furthermore, expression of in/active GSK-3β was not able to increase microtubule unbundling beyond the levels of homozygous *shot* mutants (Fig.4B). This suggests that Shot and GSK-3β act within the same pathway. We next wanted to test if this is a direct interaction and tested if *Drosophila* Shot is a GSK-3β target.

<u>Shot C-terminus can be phosphorylated by GSK-3β</u>

The consensus target sites of GSK-3β substrates is a series of Ser/Thr–X–X–X-Ser/Thr-P motifs where serines or threonines, spaced by any three amino acids are phosphorylated progressively by the kinase. Some GSK-3β targets require phosphorylation of the first serine by a priming kinase, other, unprimed targets do not [60].

In ACF7, GSK-3β phosphorylates a cluster of serines that follow the standard GSK-3β target site pattern (Fig.4C). They are located in between the C-terminal microtubule binding domain (Gas domain) and Eb protein-binding SxIP sites. Our in-silico analysis of the Shot C-terminus identified a putative GSK-3β phosphorylation site cluster in the region, C-terminal of the microtubule-binding Gas, in between the three S-x-I/L-P motifs (Fig.4C).

To test if GSK-3β is able to phosphorylate this cluster in vitro, we generated two GST-tagged peptide versions of this target site; the wildtype sequence and a version where all Serines were mutated to alanines (serving as a negative control, Fig.4D). The well-established GSK-3β target site of MAP1B (ERLSPAKSPSLSPSPPSPIEKT; [11]) served as positive control and GST alone as negative control. We detected phosphorylated peptides that were incubated with purified human GSK-3β and ATPγS using a thiophosphate ester antibody (see Methods). Whilst the

wildtype GSK-3β sequence shows a clear phosphorylation signal, the S>A variant does not (Fig.4D',D''). This clearly shows that GSK-3β can phosphorylate the putative GSK-3β target site, potentially without requiring a priming kinase.

Phosphodeficient but not -mimetic Shot leads to microtubule unbundling

Having established that GSK-3β can phosphorylate Shot, we next wanted to test whether this has relevance in neurons. For this, we generated three fly lines where the *shot* locus is modified using CRISPR/Cas9 (Fig.5A): i) a control line where we replace the final five *Shot* exons with a fused version of those exons and an additional C-terminal GFP to visualise endogenous Shot, ii) a phosphodeficient version following the same strategy where we replaced the seven serines in the GSK-3β target site (Fig.4C) with alanine residues and iii) a variant where those serines where replaced by aspartic acid residues, mimicking phosphorylation.

To test if phosphorylation of Shot affects its ability to bind microtubules, we cultured primary neurons for 6 HIV and visualised endogenous Shot. Overall, Shot levels in neurons appeared to be very low with Shot localised along neurons in a punctate pattern. Co-stainings with tubulin show that the majority of wildtype Shot localises along microtubules. Our attempts to quantify Shot intensity along microtubules failed because overall Shot levels were too low. However, qualitatively we found that the version mimicking phosphorylation ($Shot^{S>D}$-GFP, Fig.5B) does not appear to bind microtubules efficiently with fewer dots localising along microtubules and to areas without microtubules in neuronal (arrows in Fig.5B) as well as non-neuronal cells (arrows in Fig.5C). In contrast, phosphodeficient Shot ($Shot^{S>A}$-GFP, Fig.5B) localises along microtubules in both primary neurons and non-neuronal cells (Fig.5B,C). Those findings support our notion that Shot's ability to bind microtubules is reduced by GSK-3β phosphorylation, similar to findings of the Shot homologue ACF7 in migrating skin cells [13].

We next tested the impact of Shot phosphorylation on microtubule bundling. Culturing primary neurons from the three Shot-GFP lines for 6HIV, we found that only neurons expressing phosphodeficient $Shot^{S>A}$-GFP displayed a 2.9-fold increase in unbundled, disorganised microtubules (Fig.5D). In both, $Shot^{WT}$-GFP and $Shot^{S>D}$-GFP microtubule disorganisation was not significantly increased (Fig.5D).

There seems to be a contradiction here. Whilst phosphomimetic Shot loses its ability to bind microtubules phosphodeficient, microtubule-binding variant causes microtubule unbundling. Explanation for this could come from Shot's dual role in 1) regulating microtubule stability through MT interaction via the Gas2 (growth arrest specific 2)-related domain (GRD) domain and 2) guidance of microtubule polymerisation which is mediated by C-terminal S-x-I/L-P sites that interact with Eb1 [28]. Our findings in primary neurons would suggest that phosphodeficient $Shot^{S>A}$-GFP, but not $Shot^{S>D}$-GFP affects Shot ability to interact with Eb1. We tested this by qualitatively analysing co-localisation of Eb1 and Shot (proper quantification was here again not possible due to low Shot levels) and found that $Shot^{S>D}$-GFP appears to co-localised with Eb1, but not $Shot^{S>A}$-GFP (Fig.5E). In addition, previous work had shown that loss of Shot-Eb1 interaction leads to an increase in Eb1 comet sizes, likely due to Shot binding slowing microtubule polymerisation [28]. Eb1 comet length is increased in phosphodeficient $Shot^{S>A}$-GFP, but not $Shot^{S>D}$-GFP (Fig.5F,F'). This supports the hypothesis that Shot/Eb1 interaction is abrogated in the phosphodeficient Shot variant leading to microtubule unbundling, because the guidance function of Shot relies on this interaction.

To test further whether a shift of Shot towards an unphosphorylated state is the cause of microtubule unbundling when GSK-3β is inhibited, we treated primary neurons with endogenously modified Shot versions with the GSK-3β inhibitor Lithium. As expected,

incubation of the control line with 10uM Li leads to a 3-fold increase in microtubule unbundling (Fig.5G). However, addition of Li does not increase the degree of microtubule unbundling in Shot$^{S>A}$-GFP and, importantly, does not cause microtubule disorganisation in Shot$^{S>D}$-GFP. Those data strongly suggest that microtubule unbundling upon GSK-3β inhibition is mediated by Shot.

Discussion

A novel role of GSK-3β in maintaining microtubule bundles in axons

GSK-3β has long been known to control microtubule stability and polymerisation in various context. Here, we here describe a new, evolutionary conserved role of GSK-3β in maintaining parallel bundles of microtubules. We find that GSK-3β activity needs to be tightly balanced to maintain parallel bundles of microtubules; both over- as well as inactivation leads to curling of microtubules in fly and rat neurons.

We made use of our fly model and previous functional studies of >30 microtubule binding proteins to identify GSK-3β key targets that mediate this. Overall, we propose a model where GSK-3β affects 2/3 of the 'power trio' of microtubule polymerisation: Tau and Shot. Previous work described that both microtubule regulators have a key role in maintaining microtubule bundling through Shot/Eb1 mediated guidance of microtubule polymerisation[30]. Our data supports a model where the Shot/Eb1 link breaks in different ways when GSK-3β is inhibited or overactive. In both scenarios Shot guiding of polymerising microtubules is reduced, leading to microtubules growing towards the plasma membrane and formation of curls [30]. When GSK-3β is overactive it is mediated through Tau where Tau detaches from microtubules and does not prevent Eb1 binding. Consequently, Eb1 is sequestered to the microtubule shaft and therefore not able to form proper plus ends. GSK-3β inhibition reduces Shot's affinity to Eb1 thereby affecting Shot's microtubule guidance function. Both microtubule regulators have been characterised as GSK-3β targets previously. We did not experimentally test the third member the 'power trio', XMAP215, even though mutants show a strong microtubule unbundling phenotype, because previous work suggests that Drosophila XMAP215 (msps) is not phosphorylated by GSK-3β [61]. It is possible that the function of this key microtubule polymerase is affected, because Eb1 and XMAP215 are co-dependent at plus ends [62]. Reduction of Eb1 at plus ends observed when expressing active GSK-3β will likely affect XMAP215 binding to plus ends, increasing the impact on microtubule growth and guidance.

This new function of GSK-3β in maintaining microtubule bundles has important implications for neuronal development and maintenance. The morphology and physiology of axons crucially depends on the parallel bundles of microtubules. They are the highways for life-sustaining vesicle transport and organelle dynamics. As a consequence, microtubule bundle defects can trigger axonal decay by forming axon swellings that can lead to impaired axonal transport and action potential propagation, a key feature of axonopathies [21]. Reports of such pathological axon swellings where microtubules bundles have disintegrated into loops or waves have been observed in ageing, after injury and in certain in vivo models of axonopathies (reviewed here [22]). Therefore, we suggest that unbundling of axonal microtubules could be an additional mechanism how impaired GSK-3β activity could lead to neuronal degeneration.

Explanations how such microtubule unbundling could lead to a broad range of axonopathies was recently proposed in a novel model, the dependency cycle of local axon homeostasis. [21]. In brief, this model suggests that cellular processes in axons are linked: transport of cargo is essential for axonal function and physiology. This comes at a cost, because the movement of

motor proteins cause mechanical damage to microtubule bundles [63,64]. Cytoskeletal regulators and tubulin building blocks can repair this damage to support dynamics and stability of microtubule bundles, however, this requires axonal transport of those regulators for maintenance and physiology. Breaking the cycle at any point will weaken neuronal cell homeostasis and could lead to decay providing an explanation how the loss of seemingly unrelated proteins and processes lead to similar pathologies. This is relevant for neurodegenerative disease such as Alzheimer's and Parkinson's Disease where GSK-3β is hyperactive leading to hyperphosphorylation of Tau and the subsequent formation of neurofibrillary tangles. Much emphasis has been put on those aggregates; however, loss of endogenous Tau function might play an additional vital role. We previously showed that Tau plays an important role in microtubule polymerisation and bundle organisation by keeping Eb1 off the microtubule shaft [30]. Similarly, we find here that detachment of Tau from microtubules when GSK-3β leads to microtubule unbundling through the same mechanism. Work in flies and mouse models suggested that loss of Tau alone does not cause severe phenotypes [38 65] apart from mild behavioural and motor deficits (e.g. [66 67]. However, we find that when GSK-3β is hyperactive we lose Shot microtubule binding in addition to Tau. Shot and Tau are functionally redundant where the combined loss of the both microtubule binding proteins exceeds the impact of loss of just one exponentially, leading to severe microtubule instability, impaired transport and synapse defects [68]. Therefore, the simultaneous loss of both, Tau and Shot, from microtubules could potentially have a detrimental impact on neuronal function, in addition to pathological microtubule unbundling. We therefore propose the combined loss of Tau and Shot as new mode how overactive GSK-3β leads to neuronal decay in neurodegenerative diseases.

GSK-3β phosphorylation of Shot might balance its affinity towards microtubule shaft and plus end

Our data support a model where phosphorylation by GSK-3β balances two of Shot's key functions – binding/stabilising microtubules directly and guiding microtubule polymerisation by binding Eb1 [28]. Wu et al [13]had shown previously that microtubule binding of the spectraplakin ACF7 is regulated by GSK-3β where ACF7 detaches from microtubules upon phosphorylation. We similarly see that the association of phosphomimetic *Drosophila* Shot with microtubules is reduced. However, in addition we find that Shot's interaction with Eb1 depends on its phosphorylation status with Shot still binding Eb1 even though it is detached from microtubules. This switch could represent a mechanism for how signalling coordinates and controls two key functions of Shot: Stabilising and protecting microtubules when it is unphosphorylated vs guiding polymerising microtubules into parallel bundles. A similar mechanism was described for Clasp which contains two GSK-3β motifs [69 12]. The number of phosphorylated residues determine whether it associates with the plus end, the microtubule shaft or shows no interaction with microtubules at all. In contrast to Shot, complete phosphorylation of all GSK-3β sites disrupts both the plus end-tracking and the lattice-binding activities of CLASP2 [12]. Wu et al did not analyse ACF7's interaction with Eb proteins. However, they observed that directionality of microtubule growth was largely randomized in wildtype- and KO-ACF7 cells, but not cells expressing the the phosphodeficient ACF7(S:A) variant. This might indicate that the abrogated guidance of microtubule polymerisation in unphosphorylated spectraplakins is evolutionary conserved.

We can currently only speculate how phosphorylation could determine whether Shot preferentially binds microtubules or Eb1. Our structural *in silico* analysis suggests that a key GSK-3β target cluster is in a linker region between Shot's three SxIP sites that might sit between two associated Eb1 molecules. Increasing the negative charge in this linker region might lead

to a loss of affinity for microtubules thereby strengthening interaction with Eb1. Further studies are needed to investigate this.

GSK-3β activity in neurons needs to be tightly balanced

Our work and that of others shows that GSK-3β activity needs to be tightly balanced. Whilst it is widely established that hyperactivity impairs neuronal development and drives key features of Alzheimer's Disease (Aβ production and accumulation, formation of toxic tau species, pro-inflammatory and LTP impairments; reviewed by Lauretti et al. [6]), our work potentially explains why global inhibition of GSK-3β is ineffective as treatment option. Inhibition of GSK-3β or treatments with GSK-3β inhibitors can lead to limited regenerative outgrowth [14], reduced outgrowth [70] and defects in neuronal plasticity, such as NMJ defects in flies [71]. The correct balance between GSK-3β activation and inhibition is required to drive normal development where multiple complex regulatory layers ensure that GSK-3β regulates its substrates at the appropriate time and location. We do not yet fully understand spatiotemporal activity patterns of GSK-3β. Furthermore, the regulation of microtubule networks by GSK-3β is complex and the impact of the kinase is highly dependent on individual targets, e.g. phosphorylation of MAP1b promotes microtubule dynamics [11], inhibition of GSK-3β increase microtubule stability via Tau, CRMP2 or APC (reviewed in [1]). For others such as Clasp [12] or Shot (this study) GSK-3β activity levels determine whether they bind the microtubule shaft or plus end. To fully understand this complex regulatory network, we need combine highly tractable genetic approaches with novel tools that will allow us to study the activity patterns of GSK-3β. This is the crucial next step to explore how the complexity of GSK-3β signalling is coordinated in time and space to achieve precise control over a wide range of cellular processes in the developing and mature nervous system.

Acknowledgements

This work was made possible through support by the Leverhulme Trust (ECF-2017-247), Academy of Medical Sciences Springboard Award (SBF008\) and Royal Society Research Grant (RGS\R2\222151) to I.H., AV was funded by startup funding by University of Hull and as Postdoctoral Researcher through a BBSRC grant to Andreas Prokop (BB/P020151/1). The Manchester Bioimaging Facility microscopes used in this study were purchased with grants from the BBSRC, The Wellcome Trust and The University of Manchester Strategic Fund. Work on this project benefited from the Manchester Fly Facility, established through funds from the University and the Wellcome Trust (087742/Z/08/Z). We would like to thank Peter O'Toole, Grant Calder and Karen Hogg at the York Bioscience Technology Facility for assistance with microscopy. We thank Andreas Prokop for his incredible support and discussions throughout – this work would not have been possible without. We thank Hiro Ohkura for kindly providing DmEb1 antibody. Stocks obtained from the Bloomington *Drosophila* Stock Center (NIH P40OD018537) were used in this study.

Figures

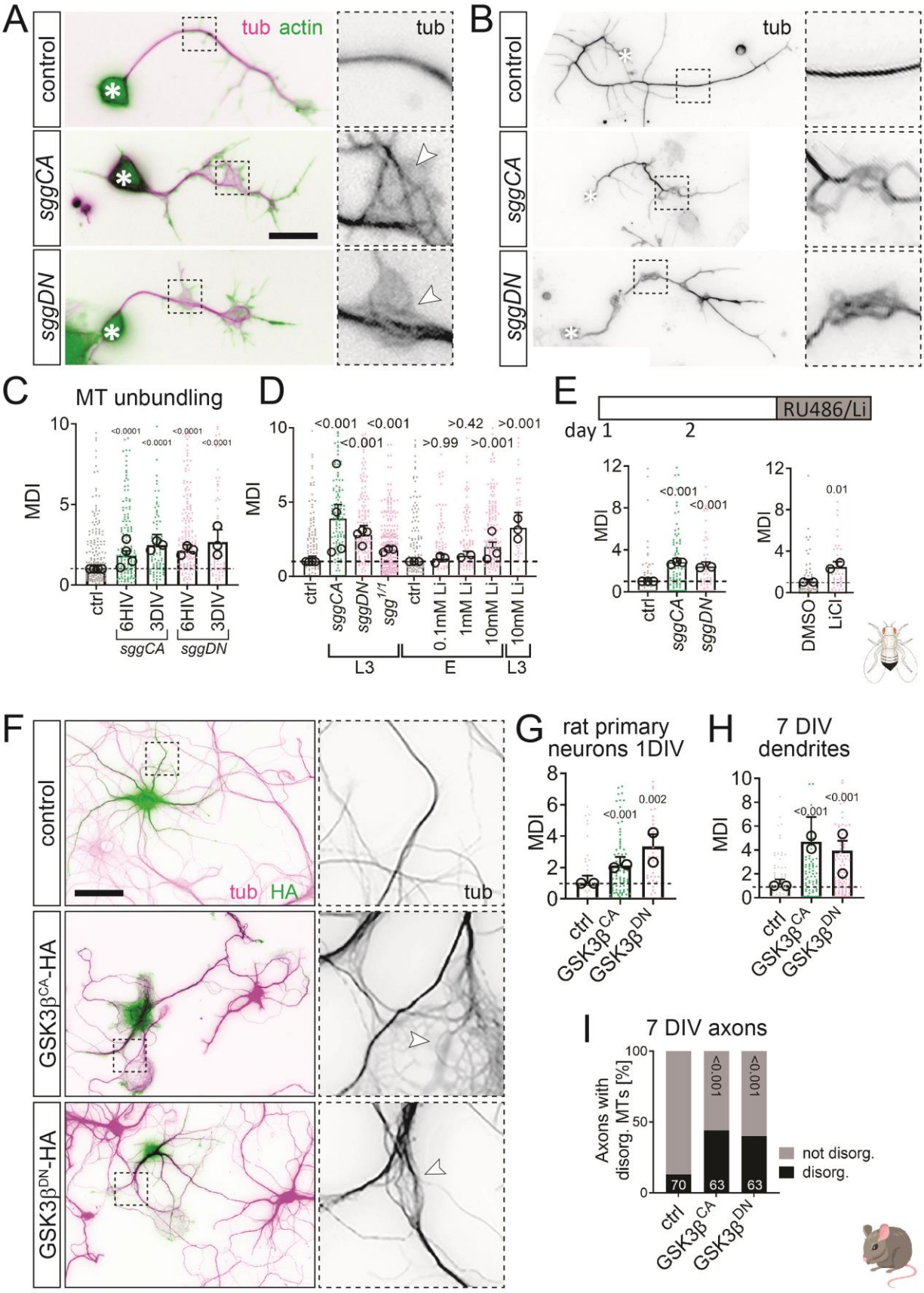

Fig. 1 Voelzmann et al

Fig 1. Inhibition and hyper-activation of GSK-3β/Shaggy both lead to curling and unbundling of axonal microtubules in *Drosophila* primary and rat hippocampal neurons.

A, B) Images of representative examples of embryonic primary neurons either immuno-stained for tubulin and actin (A) or tub (B). Neurons of the following conditions were cultured for 6 hours in vitro (6HIV, A) or 3 days in vitro (3DIV, B): controls (ctrl; elavGal4, UAS-GFP), expressing constitutively active (*sggCA*; *elavGal4, UAS-sgg*^{S9A}) or inactive (*sggDN*; *elavGal4, UAS-sgg*^{A81T}) UAS-GSK-3β variants via the pan-neuronal driver elavGal4. Asterisks indicate cell bodies, dashed squares in are shown as 3.5-fold magnified close-ups beside each image white arrow heads point at areas of microtubule curling. **C)** Quantification of microtubule unbundling depicted as MDI (see methods) obtained from embryonic primary neurons with the same genotypes as shown in A,B. **D)** Microtubule unbundling quantification of primary neurons obtained from third instar larval brains (L3) expressing in/active GSK-3β (*sggCA/DN*), embryonic primary neurons of GSK-3β mutants (*sgg*$^{1/1}$) and neurons treated with the GSK-3β inhibitor Lithium. **E)** *sggDN* or *sggCA* expression was induced via RU486 (elav::switchGal4) at 3DIV for 1DIV or control neurons were treated with 10mM Li. **F)** Images of representative examples of rat hippocampal neurons at 7 DIV expressing HA (controls), GSK-3β^{CA}-HA or GSK-3β^{DN}-HA immuno-stained for tubulin and HA. **G-I)** Quantification of microtubule unbundling depicted as MDI (G,H) or ratio (axons w/ or w/o microtubule unbundling, I) at conditions indicated above. Data were normalised to parallel controls (dashed horizontal line) and are shown as mean ± SEM; data points in each plot, taken from at least two experimental repeats consisting of 3 replicates each; large open circles in graphs indicate median/mean of independent biological repeats. P-values obtained with Kruskall-Wallis ANOVA test for the different genotypes are indicated in each graph. Scale bar in A represents 10 µm in A and 20 µm in F.

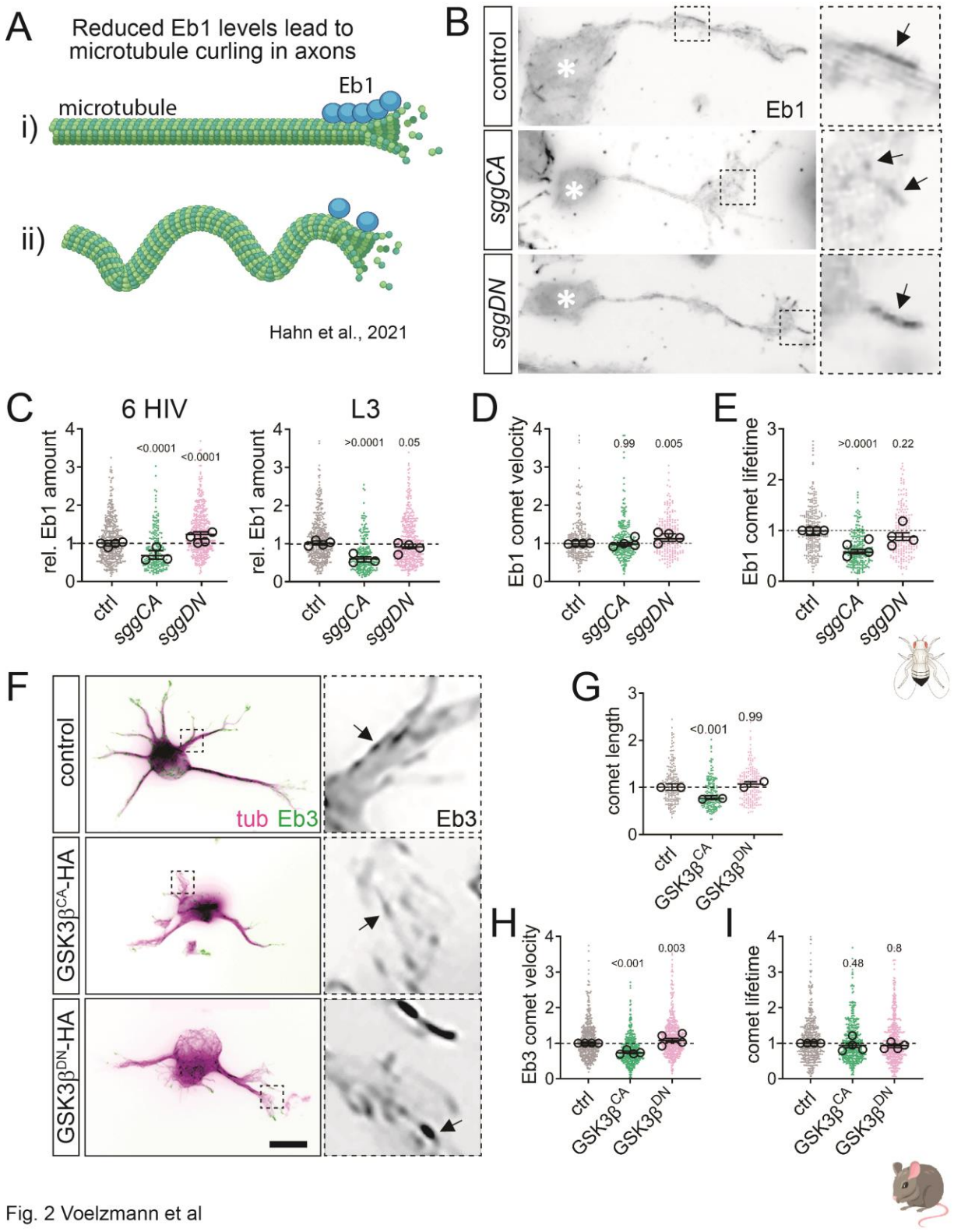

Fig. 2 Voelzmann et al

Fig 2. Expression of active GSK-3β reduces Eb1 comet size and dynamics.

A) Schematic representation how loss of Eb1 leads to microtubule unbundling: i) normal Eb1 levels support microtubule polymerisation and straight microtubule arrangement whereas ii) reduced Eb1 levels lead to microtubule curling. See Hahn et al., 2021 for details. **B)** Images of representative examples of control embryonic primary neurons or neurons expressing constitutively active (sggCA) or inactive GSK-3β (sggDN) immuno-stained for Eb1. Asterisks indicate cell bodies, dashed squares in are shown as 3.5-fold magnified close-ups beside each

image arrows point at Eb1 comets. Scale bar in B represents 10 µm. **C)** Quantification of normalised Eb1 amounts at plus ends (see Methods) obtained from embryonic primary neurons at 6HIV and larval neurons after 1 DIV (L3). **D,E)** Quantification of microtubule dynamics, i.e. comet velocity (D) and lifetime (E) in neurons expressing the GFP-tagged, plus-end binding C-tail of Shot [28] along with RFP alone (control), sggCA or sggDN. **F)** Representative images of primary rat hippocampal neurons at 1 DIV co-expressing Eb3-GFP with HA (controls), GSK-3β^{CA}-HA or GSK-3β^{DN}-HA. Asterisks indicate cell bodies, dashed squares in are shown as 3.5-fold magnified close-ups beside each image arrows point at Eb1 comets **G)** Quantification of normalised Eb1 comet lengths (see Methods) obtained from the same genotypes as shown in F. **H,I)** Quantification of microtubule dynamics, i.e. comet velocity (H) and lifetime (I) in rat hippocampal neurons expressing the GFP-tagged, plus-end binding C-tail of Shot along with RFP alone (control), GSK-3β^{CA}-HA or GSK-3β^{DN}-HA. Data were normalised to parallel controls (dashed horizontal line) and are shown as mean ± SEM; data points in each plot, taken from at least two experimental repeats consisting of 3 replicates each; large open circles in graphs indicate median/mean of independent biological repeats. P-values obtained with Kruskall-Wallis ANOVA test for the different genotypes are indicated in each graph. Scale bar in A represents 10 µm in B and 20 µm in F.

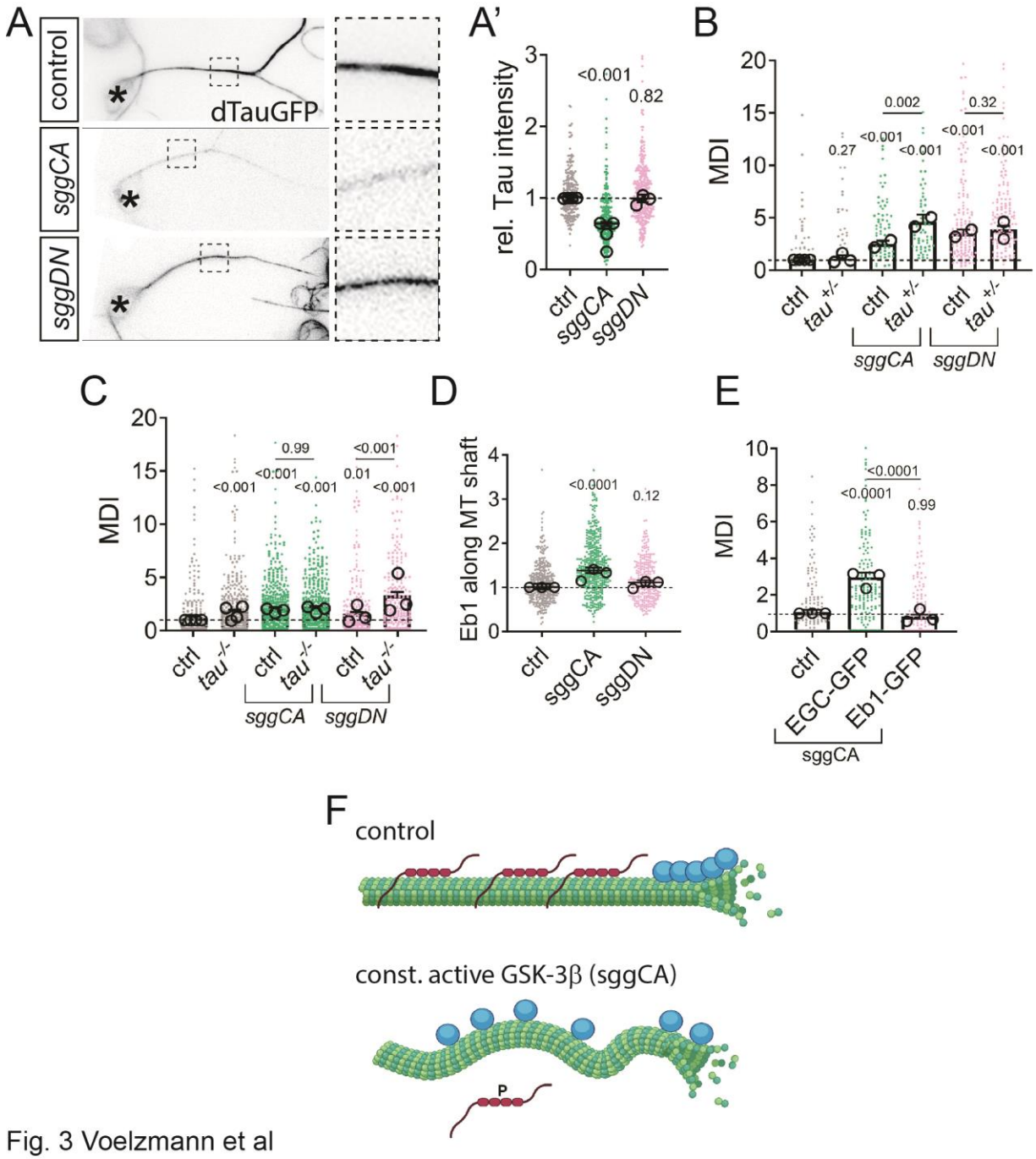

Fig. 3 Voelzmann et al

Fig. 3. Reduced Eb1 at plus ends through a loss of Tau leads to microtubule unbundling when GSK-3β is hyperactive

A) Representative images of primary neurons expressing dTau-GFP (P{Wee}tau[304]) at endogenous levels, alone or in combination with const. active (*UAS-sggCA*) or inactive (*UAS-sggDN*) GSK-3β expression. Asterisks indicate cell bodies, dashed squares are shown as 3.5-fold magnified close-ups beside each image; arrows point at axon terminals. **A')** Quantification of relative Tau mean intensity along micrtoubules for indicated conditions; data are normalised to control. **B, C)** Microtubule curling for primary neurons displaying heterozygous (B) and homozygous (C) tau^{KO} ($tau^{KO\ 38}$) mutant conditions, alone or in combination with expression of const. active (*UAS-sggCA*) or inactive (*UAS-sggDN*) GSK-3β via elavGal4. **C) D)** Relative Eb1 intensity along microtubules of neurons at 6 HIV without/with elav-Gal4-driven expression of *sggCA* or *sggDN*. **E)** Microtubule curling (MDI) in primary neurons expressing *sggCA* in combination with UAS-Eb1::GFP or -Shot-Ctail::GFP (as indicated). (B-E) All data were

normalised to parallel controls (dashed horizontal lines) and are shown as bar chart with mean ± SEM of at least two independent repeats with 3 technical replicates each; large open circles in graphs indicate mean of independent biological repeats. P-values above data points/bars were obtained with Kruskal-Wallis ANOVA tests. **F)** Model view of the results shown here; note that microtubules are depicted (green), blue circles represent Eb1 and red chains Tau; for further explanations see main text and Discussion.

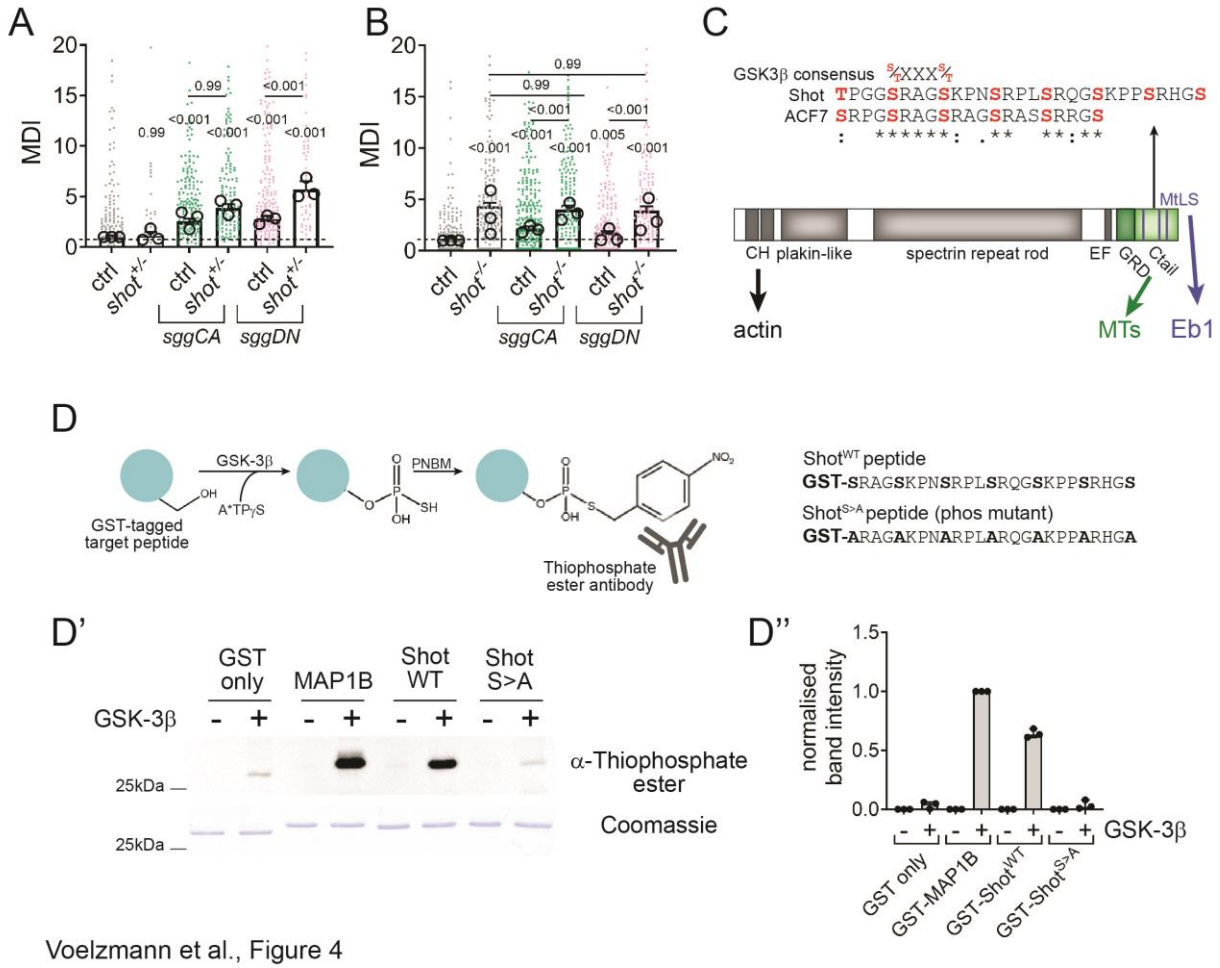

Fig. 4. The C-terminus of Shot can be phosphorylated by GSK-3β

A, B) Microtubule curling for primary neurons displaying heterozygous (A) and homozygous (B) *shot*^{3} mutant conditions, alone or in combination with expression of const. active (*UAS-sggCA*). **C)** Schematic representation of Shot; highlighting the verified ACF7 and putative Shot GSK-3β target site (consensus S/TS/T) in the C-terminal microtubule binding region. **D)** Workflow of the in vitro thiophosphorylation kinase assay and Shot^{WT} and phosphodeficient Shot$^{S>A}$ peptide sequence. D') Representative blot where phosphorylated peptides are labelled with α-Thiophosphate ester of GST control, positive control (GSK-3β target site of MAP1B,), Shot^{WT} and Shot$^{S>A}$ with or without GSK-3β. D'') Quantification of mean band intensity.

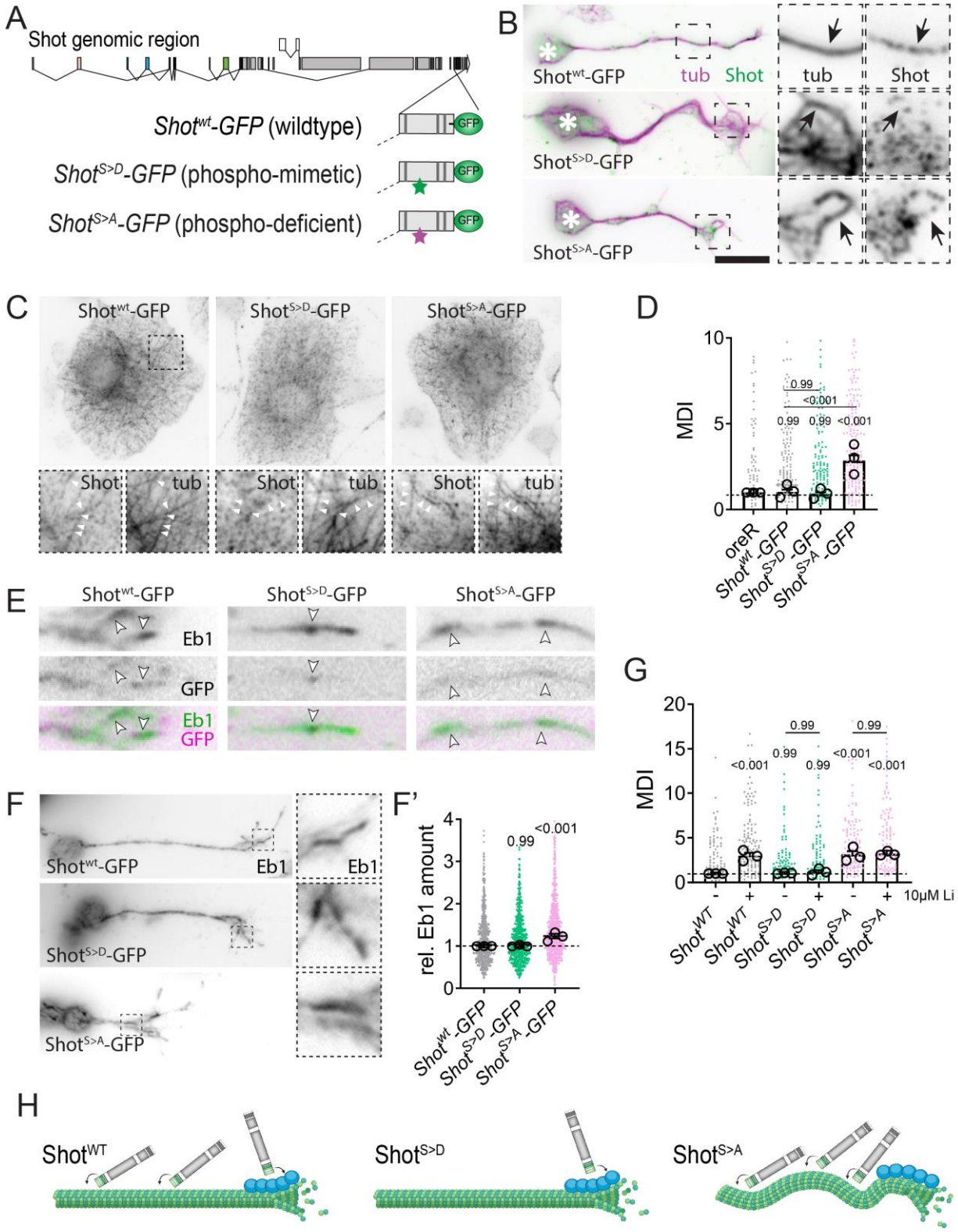

Voelzmann et al., Figure 5

Fig. 5. Phosphodeficient but not -mimetic Shot leads to microtubule unbundling

A) Schematic representation of genomic engineering approach replacing C-terminal exons of Shot to generate endongenous GFP-tagged Shot CRISPR lines, as either wildtype (*Shot^WT*), phosphomimetic (*Shot^S>D*) or -deficient (*Shot^S>A*) variants. **B, C, E, F)** Representative images of primary neurons (B) and non-neuronal cells (C) cultured for 6HIV of *Shot^WT*, *Shot^S>D* or *Shot^S>A*

labelled for tubulin (purple) and Shot (green, anti-GFP) in B, C), Eb1 in F) and Eb1 (green) and GFP (magenta) in E. Asterisks indicate cell bodies, dashed squares in are shown as 3.5-fold magnified close-ups beside (B, F) or underneath (C) each image with tubulin and GFP (Shot) channels, arrows/white arrowheads point at microtubules in B,C and at Eb1 comets in E, F. **F')** Quantification of relative Eb1 amounts at plus ends for conditions indicated. **D, G)** Quantification of microtubule unbundling (MDI) obtained from embryonic primary neurons with conditions indicated below. G) Primary neurons were treated for the entire 6HIV with 10 µM Li or vehicle. H) Cartoons illustrating current hypothesis how phosphorylation by GSK-3β affects Shot's ability to bind plus ends or microtubules.

References

1. Hur EM, Zhou FQ. GSK3 signalling in neural development. *Nat Rev Neurosci*. Aug 2010;11(8):539-51. doi:10.1038/nrn2870
2. Llorens-Martin M, Fuster-Matanzo A, Teixeira CM, et al. GSK-3beta overexpression causes reversible alterations on postsynaptic densities and dendritic morphology of hippocampal granule neurons in vivo. *Mol Psychiatry*. Apr 2013;18(4):451-60. doi:10.1038/mp.2013.4
3. Xing B, Li YC, Gao WJ. GSK3beta Hyperactivity during an Early Critical Period Impairs Prefrontal Synaptic Plasticity and Induces Lasting Deficits in Spine Morphology and Working Memory. *Neuropsychopharmacology*. Dec 2016;41(13):3003-3015. doi:10.1038/npp.2016.110
4. Rizk M, Saker Z, Harati H, Fares Y, Bahmad HF, Nabha S. Deciphering the roles of glycogen synthase kinase 3 (GSK3) in the treatment of autism spectrum disorder and related syndromes. *Mol Biol Rep*. Mar 2021;48(3):2669-2686. doi:10.1007/s11033-021-06237-9
5. Jorge-Torres OC, Szczesna K, Roa L, et al. Inhibition of Gsk3b Reduces Nfkb1 Signaling and Rescues Synaptic Activity to Improve the Rett Syndrome Phenotype in Mecp2-Knockout Mice. *Cell Rep*. May 8 2018;23(6):1665-1677. doi:10.1016/j.celrep.2018.04.010
6. Lauretti E, Dincer O, Pratico D. Glycogen synthase kinase-3 signaling in Alzheimer's disease. *Biochim Biophys Acta Mol Cell Res*. May 2020;1867(5):118664. doi:10.1016/j.bbamcr.2020.118664
7. Credle JJ, George JL, Wills J, et al. GSK-3beta dysregulation contributes to parkinson's-like pathophysiology with associated region-specific phosphorylation and accumulation of tau and alpha-synuclein. *Cell Death Differ*. May 2015;22(5):838-51. doi:10.1038/cdd.2014.179
8. Guo X, Snider WD, Chen B. GSK3beta regulates AKT-induced central nervous system axon regeneration via an eIF2Bepsilon-dependent, mTORC1-independent pathway. *Elife*. Mar 14 2016;5:e11903. doi:10.7554/eLife.11903
9. Luo J. The role of GSK3beta in the development of the central nervous system. *Front Biol (Beijing)*. Jun 2012;7(3):212-220. doi:10.1007/s11515-012-1222-2
10. Hajka D, Budziak B, Pietras L, Duda P, McCubrey JA, Gizak A. GSK3 as a Regulator of Cytoskeleton Architecture: Consequences for Health and Disease. *Cells*. Aug 14 2021;10(8)doi:10.3390/cells10082092
11. Trivedi N, Marsh P, Goold RG, Wood-Kaczmar A, Gordon-Weeks PR. Glycogen synthase kinase-3beta phosphorylation of MAP1B at Ser1260 and Thr1265 is spatially restricted to growing axons. *J Cell Sci*. Mar 1 2005;118(Pt 5):993-1005. doi:10.1242/jcs.01697
12. Hur EM, Saijilafu, Lee BD, Kim SJ, Xu WL, Zhou FQ. GSK3 controls axon growth via CLASP-mediated regulation of growth cone microtubules. *Genes Dev*. Sep 15 2011;25(18):1968-81. doi:25/18/1968 [pii] 10.1101/gad.17015911
13. Wu X, Shen QT, Oristian DS, et al. Skin stem cells orchestrate directional migration by regulating microtubule-ACF7 connections through GSK3beta. *Cell*. Feb 4 2011;144(3):341-52.
14. Gobrecht P, Leibinger M, Andreadaki A, Fischer D. Sustained GSK3 activity markedly facilitates nerve regeneration. *Nat Commun*. Jul 31 2014;5:4561. doi:10.1038/ncomms5561
15. Kim WY, Zhou FQ, Zhou J, et al. Essential roles for GSK-3s and GSK-3-primed substrates in neurotrophin-induced and hippocampal axon growth. *Neuron*. Dec 21 2006;52(6):981-96. doi:10.1016/j.neuron.2006.10.031

16. Liz MA, Mar FM, Santos TE, et al. Neuronal deletion of GSK3beta increases microtubule speed in the growth cone and enhances axon regeneration via CRMP-2 and independently of MAP1B and CLASP2. *BMC Biol*. Jun 12 2014;12:47. doi:10.1186/1741-7007-12-47
17. Duda P, Wisniewski J, Wojtowicz T, et al. Targeting GSK3 signaling as a potential therapy of neurodegenerative diseases and aging. *Expert Opin Ther Targets*. Oct 2018;22(10):833-848. doi:10.1080/14728222.2018.1526925
18. Alonso AD, Cohen LS, Corbo C, et al. Hyperphosphorylation of Tau Associates With Changes in Its Function Beyond Microtubule Stability. *Front Cell Neurosci*. 2018;12:338. doi:10.3389/fncel.2018.00338
19. Stamer K, Vogel R, Thies E, Mandelkow E, Mandelkow EM. Tau blocks traffic of organelles, neurofilaments, and APP vesicles in neurons and enhances oxidative stress. *J Cell Biol*. Mar 18 2002;156(6):1051-63. doi:10.1083/jcb.200108057
20. Arciniegas Ruiz SM, Eldar-Finkelman H. Glycogen Synthase Kinase-3 Inhibitors: Preclinical and Clinical Focus on CNS-A Decade Onward. *Front Mol Neurosci*. 2021;14:792364. doi:10.3389/fnmol.2021.792364
21. Prokop A. A common theme for axonopathies? The dependency cycle of local axon homeostasis. *Cytoskeleton (Hoboken)*. Feb 2021;78(2):52-63. doi:10.1002/cm.21657
22. Hahn I, Voelzmann A, Liew Y-T, Costa-Gomes B, Prokop A. The model of local axon homeostasis - explaining the role and regulation of microtubule bundles in axon maintenance and pathology *Neural Dev*. 2019;14(11):10.1186/s13064-019-0134-0.
23. Wirths O, Weis J, Kayed R, Saido TC, Bayer TA. Age-dependent axonal degeneration in an Alzheimer mouse model. *Neurobiol Aging*. Nov 2007;28(11):1689-99. doi:10.1016/j.neurobiolaging.2006.07.021
24. Tang-Schomer MD, Johnson VE, Baas PW, Stewart W, Smith DH. Partial interruption of axonal transport due to microtubule breakage accounts for the formation of periodic varicosities after traumatic axonal injury. *Exp Neurol*. Jan 2012;233(1):364-72. doi:10.1016/j.expneurol.2011.10.030 S0014-4886(11)00402-X [pii]

25. Tran HT, Tsai EHR, Lewis AJ, et al. Alterations in Sub-Axonal Architecture Between Normal Aging and Parkinson's Diseased Human Brains Using Label-Free Cryogenic X-ray Nanotomography. *Front Neurosci*. 2020;14:570019. doi:10.3389/fnins.2020.570019
26. Singh S, Dallenga T, Winkler A, et al. Relationship of acute axonal damage, Wallerian degeneration, and clinical disability in multiple sclerosis. *J Neuroinflammation*. Mar 17 2017;14(1):57. doi:10.1186/s12974-017-0831-8
27. Smith G, Sweeney ST, O'Kane CJ, Prokop A. How neurons maintain their axons long-term: an integrated view of axon biology and pathology. *Front Neurosci*. 2023;17:1236815. doi:10.3389/fnins.2023.1236815
28. Alves-Silva J, Sánchez-Soriano N, Beaven R, et al. Spectraplakins promote microtubule-mediated axonal growth by functioning as structural microtubule-associated proteins and EB1-dependent +TIPs (Tip Interacting Proteins). *J Neurosci*. Jul 4 2012;32(27):9143-58. doi:10.1523/JNEUROSCI.0416-12.2012 32/27/9143 [pii]

29. Sánchez-Soriano N, Travis M, Dajas-Bailador F, Goncalves-Pimentel C, Whitmarsh AJ, Prokop A. Mouse ACF7 and Drosophila Short stop modulate filopodia formation and microtubule organisation during neuronal growth. *J Cell Sci*. Jul 15 2009;122(Pt 14):2534-42. doi:10.1242/jcs.046268 122/14/2534 [pii]

30. Hahn I, Voelzmann A, Parkin J, et al. Tau, XMAP215/Msps and Eb1 co-operate interdependently to regulate microtubule polymerisation and bundle formation in axons. *PLoS Genet*. Jul 2021;17(7):e1009647. doi:10.1371/journal.pgen.1009647
31. Bottenberg W, Sánchez-Soriano N, Alves-Silva J, Hahn I, Mende M, Prokop A. Context-specific requirements of functional domains of the Spectraplakin Short stop in vivo. *Mech Dev*. 2009;126(7):489-502.
32. Qu Y, Hahn I, Webb SED, Pearce SP, Prokop A. Periodic actin structures in neuronal axons are required to maintain microtubules. *Mol Biol Cell*. 2016-01-01 00:00:00 2017;28 (2):296-308. doi:10.1091/mbc.e16-10-0727

33. Liew Y-T, Voelzmann A, Shields S, Sánchez-Soriano N, Prokop A. Understanding roles of microtubules during kinesin-1-linked axon degeneration.(in preparation).
34. Voelzmann A, Hahn I, Pearce S, Sánchez-Soriano NP, Prokop A. A conceptual view at microtubule plus end dynamics in neuronal axons. *Brain Res Bulletin*. 2016-01-01 00:00:00 2016;126(3):226-37. doi:10.1016/j.brainresbull.2016.08.006
35. Hazelett DJ, Bourouis M, Walldorf U, Treisman JE. decapentaplegic and wingless are regulated by eyes absent and eyegone and interact to direct the pattern of retinal differentiation in the eye disc. *Development*. Sep 1998;125(18):3741-51. doi:10.1242/dev.125.18.3741
36. Bourouis B. Targeted increase in Shaggy activity levels blocks wingless signaling. *Genesis*. 2002;34:99–102.
37. Heitzler P, Simpson P. The choice of cell fate in the epidermis of Drosophila. *Cell*. Mar 22 1991;64(6):1083-92. doi:10.1016/0092-8674(91)90263-x
38. Burnouf S, Gronke S, Augustin H, et al. Deletion of endogenous Tau proteins is not detrimental in Drosophila. *Sci Rep*. Mar 15 2016;6:23102. doi:10.1038/srep23102 srep23102 [pii]

39. Kolodziej PA, Jan LY, Jan YN. Mutations that affect the length, fasciculation, or ventral orientation of specific sensory axons in the Drosophila embryo. *Neuron*. 1995;15(2):273-286.
40. Luo L, Liao YJ, Jan LY, Jan YN. Distinct morphogenetic functions of similar small GTPases: Drosophila Drac1 is involved in axonal outgrowth and myoblast fusion. *Genes Dev*. 1994;8(15):1787-1802.
41. Clyne PJ, Brotman JS, Sweeney ST, Davis G. Green fluorescent protein tagging Drosophila proteins at their native genomic loci with small P elements. *Genetics*. Nov 2003;165(3):1433-41.
42. Stone MC, Roegiers F, Rolls MM. Microtubules have opposite orientation in axons and dendrites of Drosophila neurons. *Mol Biol Cell*. Oct 2008;19(10):4122-9. doi:10.1091/mbc.E07-10-1079 E07-10-1079 [pii]

43. Osterwalder T, Yoon KS, White BH, Keshishian H. A conditional tissue-specific transgene expression system using inducible GAL4. *Proc Natl Acad Sci U S A*. Oct 23 2001;98(22):12596-601.
44. Nicholson L, Singh GK, Osterwalder T, Roman GW, Davis RL, Keshishian H. Spatial and temporal control of gene expression in Drosophila using the inducible GeneSwitch GAL4 system. I. Screen for larval nervous system drivers. *Genetics*. Jan 2008;178(1):215-34. doi:10.1534/genetics.107.081968
45. Gratz SJ, Ukken FP, Rubinstein CD, et al. Highly specific and efficient CRISPR/Cas9-catalyzed homology-directed repair in Drosophila. *Genetics*. January 29, 2014 2014;10.1534/genetics.113.160713doi:10.1534/genetics.113.160713
46. Port F, Bullock SL. Augmenting CRISPR applications in Drosophila with tRNA-flanked sgRNAs. *Nat Methods*. Oct 2016;13(10):852-4. doi:10.1038/nmeth.3972
47. Prokop A, Küppers-Munther B, Sánchez-Soriano N. Using primary neuron cultures of Drosophila to analyse neuronal circuit formation and function. *The making and un-making of neuronal circuits in Drosophila*. 2012;69:225-47. Neuromethods. doi:10.1007/978-1-61779-830-6_10
48. Qu Y, Hahn I, Lees M, et al. Efa6 protects axons and regulates their growth and branching by inhibiting microtubule polymerisation at the cortex. *eLife*. 2019;8:e50319.
49. Kaech S, Banker G. Culturing hippocampal neurons. *Nat Protoc*. 2006;1(5):2406-15. doi:10.1038/nprot.2006.356
50. Rogers SL, Rogers GC, Sharp DJ, Vale RD. Drosophila EB1 is important for proper assembly, dynamics, and positioning of the mitotic spindle. *J Cell Biol*. Sep 2 2002;158(5):873-84.
51. Elliott SL, Cullen CF, Wrobel N, Kernan MJ, Ohkura H. EB1 is essential during Drosophila development and plays a crucial role in the integrity of chordotonal mechanosensory organs. *Mol Biol Cell*. Feb 2005;16(2):891-901.

52. Sánchez-Soriano N, Gonçalves-Pimentel C, Beaven R, et al. Drosophila growth cones: a genetically tractable platform for the analysis of axonal growth dynamics. *Dev Neurobiol*. 2010;70(1):58-71.
53. Bourouis M, Moore P, Ruel L, Grau Y, Heitzler P, Simpson P. An early embryonic product of the gene shaggy encodes a serine/threonine protein kinase related to the CDC28/cdc2+ subfamily. *EMBO J*. Sep 1990;9(9):2877-84. doi:10.1002/j.1460-2075.1990.tb07477.x
54. Stambolic V, Ruel L, Woodgett JR. Lithium inhibits glycogen synthase kinase-3 activity and mimics wingless signalling in intact cells. *Curr Biol*. Dec 1 1996;6(12):1664-8. doi:10.1016/s0960-9822(02)70790-2
55. Robles-Murguia M, Hunt LC, Finkelstein D, Fan Y, Demontis F. Tissue-specific alteration of gene expression and function by RU486 and the GeneSwitch system. *NPJ Aging Mech Dis*. 2019;5:6. doi:10.1038/s41514-019-0036-8
56. Küppers-Munther B, Letzkus J, Lüer K, Technau G, Schmidt H, Prokop A. A new culturing strategy optimises Drosophila primary cell cultures for structural and functional analyses. *Dev Biol*. 2004;269:459-478.
57. Stambolic V, Woodgett JR. Mitogen inactivation of glycogen synthase kinase-3 beta in intact cells via serine 9 phosphorylation. *Biochem J*. Nov 1 1994;303 (Pt 3)(Pt 3):701-4. doi:10.1042/bj3030701
58. Hughes K, Nikolakaki E, Plyte SE, Totty NF, Woodgett JR. Modulation of the glycogen synthase kinase-3 family by tyrosine phosphorylation. *EMBO J*. Feb 1993;12(2):803-8. doi:10.1002/j.1460-2075.1993.tb05715.x
59. Avery L, Wasserman S. Ordering gene function: the interpretation of epistasis in regulatory hierarchies. *Trends Genet*. Sep 1992;8(9):312-6. doi:10.1016/0168-9525(92)90263-4
60. Doble BW, Woodgett JR. GSK-3: tricks of the trade for a multi-tasking kinase. *J Cell Sci*. Apr 1 2003;116(Pt 7):1175-86. doi:10.1242/jcs.00384
61. Trogden KP, Rogers SL. TOG Proteins Are Spatially Regulated by Rac-GSK3beta to Control Interphase Microtubule Dynamics. *PLoS One*. 2015;10(9):e0138966. doi:10.1371/journal.pone.0138966
62. Currie JD, Stewman S, Schimizzi G, Slep KC, Ma A, Rogers SL. The microtubule lattice and plus-end association of Drosophila Mini spindles is spatially regulated to fine-tune microtubule dynamics. *Mol Biol Cell*. Nov 2011;22(22):4343-61. doi:mbc.E11-06-0520 [pii]

10.1091/mbc.E11-06-0520
63. Andreu-Carbo M, Fernandes S, Velluz MC, Kruse K, Aumeier C. Motor usage imprints microtubule stability along the shaft. *Dev Cell*. Jan 10 2022;57(1):5-18 e8. doi:10.1016/j.devcel.2021.11.019
64. Budaitis BG, Badieyan S, Yue Y, et al. A kinesin-1 variant reveals motor-induced microtubule damage in cells. *Curr Biol*. Jun 6 2022;32(11):2416-2429 e6. doi:10.1016/j.cub.2022.04.020
65. van Hummel A, Bi M, Ippati S, et al. No Overt Deficits in Aged Tau-Deficient C57Bl/6.Mapttm1(EGFP)Kit GFP Knockin Mice. *PLoS One*. 2016;11(10):e0163236. doi:10.1371/journal.pone.0163236
66. Ikegami S, Harada A, Hirokawa N. Muscle weakness, hyperactivity, and impairment in fear conditioning in tau-deficient mice. *Neurosci Lett*. Feb 4 2000;279(3):129-32. doi:10.1016/s0304-3940(99)00964-7
67. Goncalves RA, Wijesekara N, Fraser PE, De Felice FG. Behavioral Abnormalities in Knockout and Humanized Tau Mice. *Front Endocrinol (Lausanne)*. 2020;11:124. doi:10.3389/fendo.2020.00124
68. Voelzmann A, Okenve-Ramos P, Qu Y, et al. Tau and spectraplakins promote synapse formation and maintenance through Jun kinase and neuronal trafficking. *eLife*. 2016;5:e14694.
69. Kumar P, Lyle KS, Gierke S, Matov A, Danuser G, Wittmann T. GSK3beta phosphorylation modulates CLASP-microtubule association and lamella microtubule attachment. *J Cell Biol*. Mar 23 2009;184(6):895-908.

70. Owen R, Gordon-Weeks PR. Inhibition of glycogen synthase kinase 3beta in sensory neurons in culture alters filopodia dynamics and microtubule distribution in growth cones. *Mol Cell Neurosci*. Aug 2003;23(4):626-37. doi:10.1016/s1044-7431(03)00095-2

71. Franco B, Bogdanik L, Bobinnec Y, et al. Shaggy, the Homolog of Glycogen Synthase Kinase 3, controls neuromuscular junction growth in Drosophila. *J Neurosci*. 2004;24(29):6573-6577.